Synthesis and Molecular Docking Studies of Pyrano[2,3-c] Pyrazole-3-Carboxylates as Potential Inhibitors of *Plasmodium Falciparum*

Mohd Asyraf Shamsuddin[1], Nur Hanis Zakaria[1], Mohd Fazli Mohammat[2], Jufrizal Syahri[3], Jalifah Latip[1] & Nurul Izzaty Hassan[1*]

[1]Department of Chemical Sciences, Faculty of Science and Technology
Universiti Kebangsaan Malaysia, 43600 UKM Bangi, Selangor, Malaysia
[2]Institute of Science, Level 3, Block C, Universiti Teknologi MARA, 40450 Shah Alam, Selangor, Malaysia
[3]Department of Chemistry, Universitas Muhammadiyah Riau, Jalan Tuanku Tambusai Ujung, Pekanbaru, Indonesia
[*]Corresponding author (e-mail: drizz@ukm.edu.my)

Plasmodium falciparum is the most virulent species of human malaria. Widespread resistance by *Plasmodium* parasites to quinolone based antimalarials and decreased efficacy of artemisinin-based combination therapy necessitates the discovery of new drugs. Malaria parasite enzyme in glycolytic pathway, *Plasmodium falciparum* lactate dehydrogenase (*Pf*LDH) is specially targeted for anti-malarial drugs development as it an essentials enzyme for parasite survival. Five pyrano[2,3- c]pyrazole-3-carboxylates (**1a-e**) were synthesized and subjected to molecular docking studies to identify molecular interactions between the compounds and the *Plasmodium falciparum* lactate dehydrogenase (*Pf*LDH) enzyme (PDB ID: 2A94). However, these compounds showed lower docking scores than the NADH cofactor, predicting its inefficiency in inhibiting *Pf*LDH in the glycolysis reaction. The pharmacokinetics and drug-likeness of the test compounds were subsequently computed by ADMET prediction. Most of the compounds demonstrated low central nervous system side effects, absence of potential cardiac toxicity, and passing Lipinski's five rule. These *in silico* data suggest the potentiality of pyranopyrazole derivatives to be exploited as orally safe active drugs.

Key words: Pyranopyrazole; molecular docking; *Plasmodium falciparum*; *Pf*LDH; ADMET

Received: May 2020; Accepted: June 2020

Malaria is one of the dangerous diseases that could threaten the lives of humans and other mammalian species. Most tropical and subtropical regions like Asia, America, and Africa have encountered this type of disease. Four species of the *Plasmodium* genus causing the disease are *Plasmodium falciparum*, *Plasmodium vivax*, *Plasmodium ovale*, and *Plasmodium malariae* [1]. It has been reported that *Plasmodium falciparum* is a significant and dangerous protozoan parasite in the *Plasmodium* genus [2]. Malaria is spread in humans through the Anopheles mosquito. An Anopheles mosquito will introduce *Plasmodium* sporozoites into a victim through the blood-feeding process [3]. The victim may experience fever, headache, chills, muscular aching, vomiting, cough, diarrhea, and abdominal pain.

Many malaria control strategies have been implemented, but none are suitable and cost-effective. The high cost and difficulty of transporting the drug to the rural areas worsen the problem. Besides, the elimination of this disease from an infected person is not easy. Resistance of *Plasmodium* strain towards existing drugs has caused an increase in death rates and the increase of new cases. This disease can become more complex; in which it can fend off the human immune system. Resistance is thought to be a result of mutations in the active sites of the drug target Therefore, by identifying the main targets of the drugs and fully understand the mechanism of action with respect to these targets, new and better antimalarial may be developed with a goal to overcome drug resistance. Amongst the emerging targets for antimalarial drug developments, are the enzymes of the glycolytic pathway. Thus, it is interesting to expand the search of new antimalarial designing potentials compound targeting this enzyme. Designing new chemical scaffolds with possible new mechanisms of actions have become an interesting direction for malaria chemotherapy.

Plasmodium's primary energy source is glucose [4], and thus glycolytic pathways are potential vital drug targets [5]. Glycolytic enzymes become promising targets for evolving new antimalarial drugs due to the parasite's dependence on glycolysis for energy. Lactate dehydrogenase is an essential glycolytic enzyme that ensures the regeneration of NAD^+ from NADH to carry out further glycolysis. Glycolysis reaction needs NAD^+ to accept electrons for a particular reaction. NAD^+ is an essential enzyme cofactor in cellular processes [6].

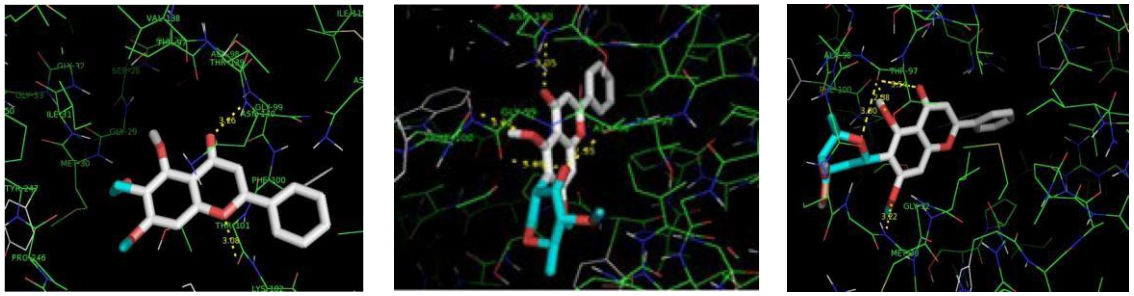

(a) (b) (c)

Figure 1. Molecular interactions between (a) Hoslundal, (b) Hoslundin, and (c) Hoslunddiol with *Pf*LDH

Chloroquine can act as a competitive inhibitor in which it competes with NADH for binding to the enzyme [7]. The glycolysis cycle is discontinued in the absence of NAD^+ in living cells. **Figure 1** shows antimalarial compounds' interactions, namely Hoslundal, Hoslunddiol, and Hoslundin, with *Pf*LDH. It can be concluded that the number of hydrogen bonds does not affect the binding energy, and a high number of hydrogen bonds from NADH to *Pf*LDH may reduce the binding affinity of other ligands to *Pf*LDH [5].

The pyranopyrazole-based compounds are recognized for several biological activities such as anticancer, antibiotic, antimalarial, and enzyme inhibitor properties [8]. The continuation of exploring the pyranopyrazole-based compounds has been attractive due to the broad spectrum of their biological activities as analgesics, anti-inflammatory, anti-bacterial, antifungal, antitubercular, antitumor, antioxidant, antiproliferative, and antihypertensive [9]. The synthesis of pyrano[2,3-*c*]pyrazoles derivatives can be achieved starting with a reaction of equimolar amounts of aldehyde, hydrazine hydrate, ethyl acetoacetate, and malononitrile in the presence of catalytic amounts of sodium benzoate in an aqueous medium at room temperature [10]. A series of substituted aromatic aldehyde and phenylhydrazine was used to explore the synthesis reaction, which yielded a total of 17 derivatives. **Figure 2** illustrates the reaction to synthesize pyranopyrazole using sodium benzoate as a catalyst.

In pursuit of developing a green and economical synthesis of pyranopyrazole, Sonar *et al*. (2018) successfully prepared pyrano[2,3-c]pirazole derivative compounds using a one-pot three-component synthesis [11]. It was reported that the three components used were aromatic aldehyde, malononitrile, and 3-methyl-1H-pyrazole-5(4H)-one, with triethanolamine as a catalyst (**Figure 3**).

In this study, five pyrano[2,3-c]pyrazole-3-carboxylate derivatives were obtained via multicomponent reactions of diethyl oxaloacetate, hydrazine, aldehyde, and malononitrile in refluxing ethanolic solutions as described by Mohammat *et al*. (2018) [12]. Subsequently, the synthesized pyrano[2,3-c]pyrazole derivatives were subjected to molecular docking studies to identify potential inhibitors of *Plasmodium falciparum* lactate dehydrogenase (*Pf*LDH) enzyme (PDB ID: 2A94) using the CDOCKER program. We also calculated the different pharmacokinetic parameters and drug-like properties of the compounds using Absorption, Distribution, Metabolism, Excretion, and Toxicity (ADMET) predictions.

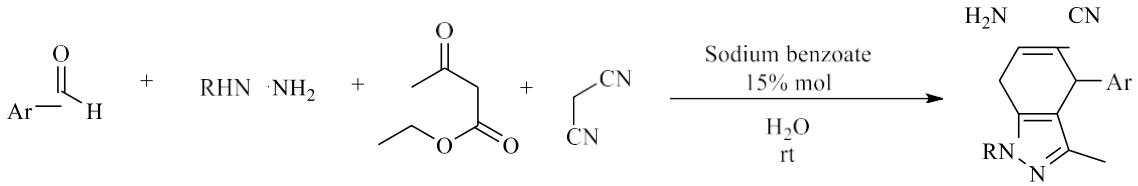

Figure 2. Reaction scheme of the synthesis of pyrano[2,3-c]pyrazole using sodium benzoate as a catalyst

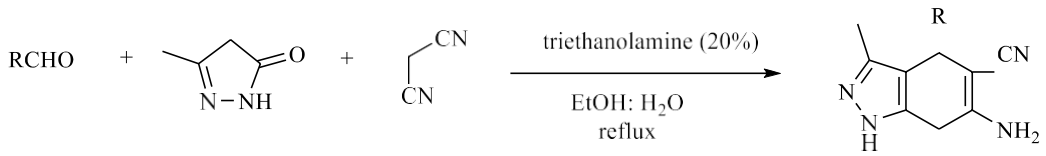

Figure 3. Reaction scheme of the synthesis of pyranopyrazole using triethanolamine as a catalyst

MATERIALS AND METHODS

Chemicals

Diethyloxalacetate sodium salt(95%, Sigma Aldrich), malononitrile(99%, Sigma Aldrich), hydrazine hydrate (≥80%, Sigma Aldrich), acetic acid(98%, Friendemann Schmidt), benzaldehyde(99%, Acros Organic), 4-Methoxy benzaldehyde(99%, Acros Organic), 4- Hydroxybenzaldehyde(99%, Acros Organic),Furan-2-carbaldehyde(99%, Acros Organic), isobutyraldehyde(99%, Acros Organic), ethanol (Acros Organic), and diethyl ether(Sigma Aldrich were purchased and used without further purification unless stated.

Instruments

The progress of the reactions was monitored by thin-layer chromatography (Merck Kiesel 60 F254, 0.25 mm thickness), and the compounds were purified by silica gel column chromatography. ^{1}H-NMR (400 MHz) and ^{13}C-NMR (100 MHz) spectra were recorded on a JEOL Resonance ECZ400S instrument using $CDCl_3$ or DMSO-d_6 as a solvent with TMS as an internal reference. The chemical shift values are expressed on the δ scale, and the coupling constant (*J)* is in Hz. Melting points were recorded on Stuart SMP40 melting point apparatus and uncorrected. Carbon, hydrogen, and nitrogen elemental analyses were analyzed using Flash Elemental Analyzer 110 series. IR spectra were recorded on Varian Excalibur 3100 FTIR spectrometer.

Molecular Docking studies

The *in silico* study was divided into two main steps. The first step was preparing the protein and ligand interaction, and the second step was docking analysis between the target protein and ligands of the compounds. The best protein crystal to be used in the *in silico* study, among all in the Protein Data Bank list, was PDB ID: 2A94, in which it has the lowest energy and maximum stability [13]. The three-dimensional protein crystal structure of *Pf*LDH, which has a resolution of 1.7 Å, R value-free: 0.167, and R-value work of 0.142, was retrieved from the RSCB Protein Data Bank and used for the docking studies. Any unnecessary chains, water that does not interact with the ligand, and unneeded cofactors from the protein crystal retrieved were cleaned. Grid generation was applied to find the active site of the protein. The ligands applied in this study were the chemical structures of the derivatives of pyrano[2,3-c]pyrazole-3-carboxylate, **1a-e.**

CDOCKER docking program

The CDOCKER docking was performed following the standard protocol implemented in Discovery Studio® 3.1 (Accelrys, San Diego, USA). Initially, the protein crystal structure was reiterated before the docking process. The ligands were prepared and minimized by adding hydrogen atoms to the protein structure, and all ionizable residues were set at their default protonation, pH 7.4. During the docking process, the receptor was held rigid while the ligands were allowed to flex during refinement. Several polar or nonpolar receptor hotspots for conformer matching starting were set at 500 with the docking tolerance of 0.25 Å. The ligands' conformation generation was set at 500, within the relative energy threshold of 20 kcal/mol [14].

GLIDE docking program

The tested compounds were constructed and optimized using ChemDraw Ultra 12.0. The optimized geometry structures were saved in a .cdx file format. The optimum pH for the compounds was set to 7.8 and set to desalt. All combination stereoisomers of the compounds to dock with the target were generated. Rigid docking was carried out against *Pf*LDH protein using GLIDE (Schrödinger, New York). The results of docking were analyzed and submitted for ADMET prediction.

Lipinski's rule of five predictions

The *Sanjeevini* web server and ChemDraw Professional 15.0 software were used to calculate and probe the value of Log P and hydrogen bond donors and acceptors and the molecular weight based on Lipinski's rule of five as described in the reported procedure [15].

General Procedure for the Synthesis of Pyrano[2,3-c]pyrazole (1a-e)

Target compounds **1a-e** were obtained in moderate to excellent yields following the procedures developed by Muhammat *et al*. (2018) [12]. In a 100 mL round-bottom flask, diethyloxalacetate sodium salt (1.16 g, 5.5 mmol), hydrazine hydrate 80% (0.2 mL, 5.5 mmol), 1 mL of acetic acid, and 30 mL of ethanol as a solvent were all added together. Reaction mixture was heated at 120ºC for 30 min.

After that, malononitrile (0.33 g, 5 mmol) and benzaldehyde (0.32 mL, 5 mmol) were then added. The reaction was continuously heated for 45 min, and TLC routinely checked the progress of the reaction. Spots were visualized by short-wave UV light. After completion, the reaction mixture was cooled to room temperature, and the precipitate formed was washed with water, dried, and recrystallized from ethanol (**Figure 4**). Their analytical and spectral data were in agreement with previously published data.

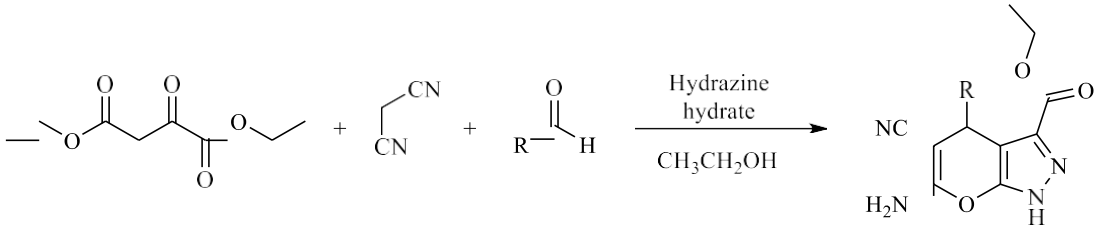

Figure 4. A synthesis scheme of pyranopyrazole derivatives. R= (a) benzaldehyde, (b) ethyl benzaldehyde, (c) furan-2-carbaldehyde, (d) isobutyraldehyde, and (e) 4-hydroxybenzaldehyde

*Synthesis of Ethyl 6-amino-5-cyano-4-phenyl-1,4-dihydropyrano[2,3-c]pyrazole-3-carboxylate (**1a**)*

Colorless powder, m.p.: 215-216ºC, yield 55%; IR cm^{-1}: 3388 (NH_2), 3218 (NH), 2199 (CN), 1716 (COOEt), 1651 (C=C); ^{1}H-NMR (400 MHz, DMSO-d_6) δ 7.24 (t, J = 7.3 Hz, 2H), 7.16 (d, J = 7.3 Hz, 1H), 7.05 (d, J = 7.3 Hz, 2H), 7.00 (s, 2H), 4.71 (s, 1H), 4.04 (q, J = 7.0 Hz, 2H), 1.00 (t, J = 7.1 Hz, 3H); ^{13}C-NMR (100 MHz, DMSO-d_6): 160.5 (CNH_2), 158.6 (C=O), 156.1 (CNH), 145.4 (quat. Ar C), 129.5 (C=N), 128.7 (Ar C), 127.8 (Ar C), 127.1 (Ar C), 120.8 (CN), 104.1 (quat. C), 61.3 (CH_2), 58.3 (quat. C), 37.5 (CH), 14.3 (CH_3); Anal. calc. for $C_{16}H_{14}N_4O_3$ C 61.93, H 4.55, N 18.06. Found: C 62.04, H 4.52, N 20.83.

*Synthesis of Ethyl 6-amino-5-cyano-4-(4-ethylphenyl)-1,4-dihydropyrano[2,3-c]pyrazole-3-carboxylate (**1b**)*

Colorless powder, m.p.: 216-217ºC, yield 50%; IR cm^{-1}: 3433 (NH_2), 3155 (NH), 2194 (CN), 1727 (COOEt), 1631 (C=C); ^{1}H-NMR (400 MHz, DMSO-d_6) δ 7.07 (d, J = 8.2 Hz, 2H), 6.95 (m, 4H), 4.67 (s, 1H), 4.12-4.02 (m, 2H), 2.51 (q, J = 7.5 Hz, 2H), 1.10 (t, J = 7.5 Hz, 3H), 1.01 (t, J = 7.1 Hz, 3H); ^{13}C-NMR (100 MHz, $CDCl_3$): δ 14.3, 16.0, 28.3, 37.1 58.5, 61.3, 104.4, 120.9, 127.7, 128.1, 129.5, 142.5, 142.8, 156.1, 158.7, 160.5; Anal. calc. for $C_{18}H_{18}N_4O_3$ C 63.89, H 5.36, N 16.56. Found: C 64.46, H 5.41, N 18.71.

*Synthesis of Ethyl 6-amino-5-cyano-4-(furan-2-yl)-1,4-dihydropyrano[2,3-c]pyrazole-3-carboxylate (**1c**)*

Brown powder, m.p.: 218-219ºC, yield 61%; IR cm^{-1}: 3404 (NH_2), 3298 (NH), 2192 (CN), 1713 (COOEt), 1644 (C=C); ^{1}H-NMR (400 MHz, DMSO-d_6) δ 7.44 (dd, J = 1.8, 0.9 Hz, 1H), 7.08 (s, 2H), 6.31 (dd, J = 3.2, 1.8 Hz, 1H), 6.07 (d, J = 2.7 Hz, 1H), 4.88 (s, 1H), 4.25-3.82 (m, 2H), 1.12 (t, J = 7.1 Hz, 3H); ^{13}C-NMR (100 MHz, $CDCl_3$): δ 14.4, 31.2, 56.3 61.5, 101.5, 105.9, 110.9, 120.7, 129.8, 142.8, 155.9, 158.8, 161.3; Anal. calc. for $C_{14}H_{12}N_4O_4$ C 56.00, H 4.03, N 18.66. Found: C 56.29, H 4.04, N 21.32.

*Synthesis of Ethyl 6-amino-5-cyano-4-isopropyl-1,4-dihydropyrano[2,3-c]pyrazole-3-carboxylate (**1d**)*

Yellow solid, m.p.: 196-197ºC, yield 30%; IR cm^{-1}: 3427 (NH_2), 3178 (NH), 2192 (CN), 1712 (COOEt), 1633 (C=C); ^{1}H-NMR (400 MHz, DMSO-d_6) δ 6.97 (s, 2H), 4.43-4.10 (m, 2H), 3.58 (d, J = 3.0 Hz, 1H), 2.10-1.85 (m, 1H), 1.27 (t, J = 7.1 Hz, 3H), 0.94 (d, J = 6.9 Hz, 3H), 0.57 (d, J = 6.9 Hz, 3H); ^{13}C-NMR (100 MHz, $CDCl_3$): δ 14.5, 17.2, 20.7, 35.7, 37.6, 51.8, 61.5, 105.3, 122.3, 128.7, 156.9, 159.1, 163.5; Anal. calc. for $C_{13}H_{16}N_4O_3$ C 56.51, H 5.84, N 20.28. Found: C 56.18, H 5.85, N 21.93.

*Synthesis of Ethyl 6-amino-5-cyano-4-(4-hydroxyphenyl)-1,4-dihydropyrano[2,3-c]pyrazole-3-carboxylate (**1e**)*

Colorless powder, m.p.: 210-211ºC, yield 44%; IR cm^{-1}: 3406 (NH_2), 3222 (NH), 2273 (CN), 1731 (COOEt), 1650 (C=C); ^{1}H-NMR (400 MHz, DMSO-d_6) δ 9.21 (s, 1H), 6.90 (s, 2H), 6.84 (d, J = 8.7 Hz, 2H), 6.61 (d, J = 8.7 Hz, 2H), 4.59 (s, 1H), 4.07 (q, J = 7.2 Hz, 2H), 4.00 (s, 1H), 1.06 (t, J = 7.1 Hz, 3H); ^{13}C-NMR (100 MHz, $CDCl_3$): δ 14.3, 36.7, 58.9, 61.3, 104.8, 115.4, 120.9, 128.8, 135.9, 137.7, 156.5, 158.7, 160.4; Anal. calc. for $C_{16}H_{14}N_4O_4$ C 58.89, H 4.32, N 17.70. Found: C 58.91, H 4.31, N 19.73.

RESULTS AND DISCUSSION

The synthesis of pyrano[2,3-c]pyrazole-3-carboxylate derivatives was conducted through a four-component reaction, which consisted of diethyloxalacetate sodium salt, hydrazine, benzaldehyde, malononitrile in ethanol, and acetic acid as a catalyst. The characteristic IR vibrations for compounds **1a-e** were the ester group (1712-1731 cm^{-1}), CN (2192-2273 cm^{-1}), NH (3178-3222 cm^{-1}), NH_2 (3388-3433 cm^{-1}), and C=C stretching (1633-1651 cm^{-1}). Among the characteristic signals in the ^{1}H-NMR spectra of the pyranopyrazole derivatives (**1a-e**) were the resonances of the ester group (1.15 and 4.00 ppm), singlets of protons of NH_2 groups (6.90 ppm), and the respective signals of aromatic protons (~ 6.60 ppm). **Figure 5** shows the ^{1}H and ^{13}C-NMR spectra of compound **1b**. The peaks at 1.01 and 1.10 ppm in the ^{1}H-NMR spectrum corresponded to the terminal methyl groups (-CH_3), while the methylene groups (-CH_2) of the ethylphenyl moiety occurred as a quartet at 2.51 ppm. The proton attached to carbon 5 was featured as a singlet at 4.67 ppm. Peaks at 7.70 and 6.95 ppm were related to the aromatic protons and primary amine protons, respectively. In the ^{13}C-NMR spectrum, the carbonyl group (-CO-) of the ester

appeared at 160.5 ppm, whereas the methoxy carbon (-OCH_3-) could be seen at 58.5 ppm. The nitrile carbon was present at 120.9 ppm, and peaks of aromatic carbons could be observed at 127.7 and 128.1 ppm. Besides, peaks at 61.3-28.3 ppm and 14.3-16.0 ppm corresponded to the –CH_2- and terminal –CH_3- groups of compound **1b**.

The reaction mechanism of compound **1a** via two parallel reactions using acetic acid as a catalyst can be visualized in **Figure 6**. Hydrazine hydrate has a robust nucleophilic group (NH_2) capable of reacting with the carbonyl group of dietyloxaloactetate sodium salt, giving pyrazolone intermediate (red box). It was found that acetic acid functioned as a catalyst in mediating the reaction and assisting the solubility of diethyloxalacetate sodium salt in ethanol. Concurrently, water deprotonated malononitrile to give a carbanion species, capable of reacting with the aldehyde group to give 2-benzylidenemalono- dinitrile intermediate (blue box). Subsequently, pyrazolone and arylidenemalono-dinitrile reacted with each other, followed by isomerization and cyclization to furnish compound **1a** [16].

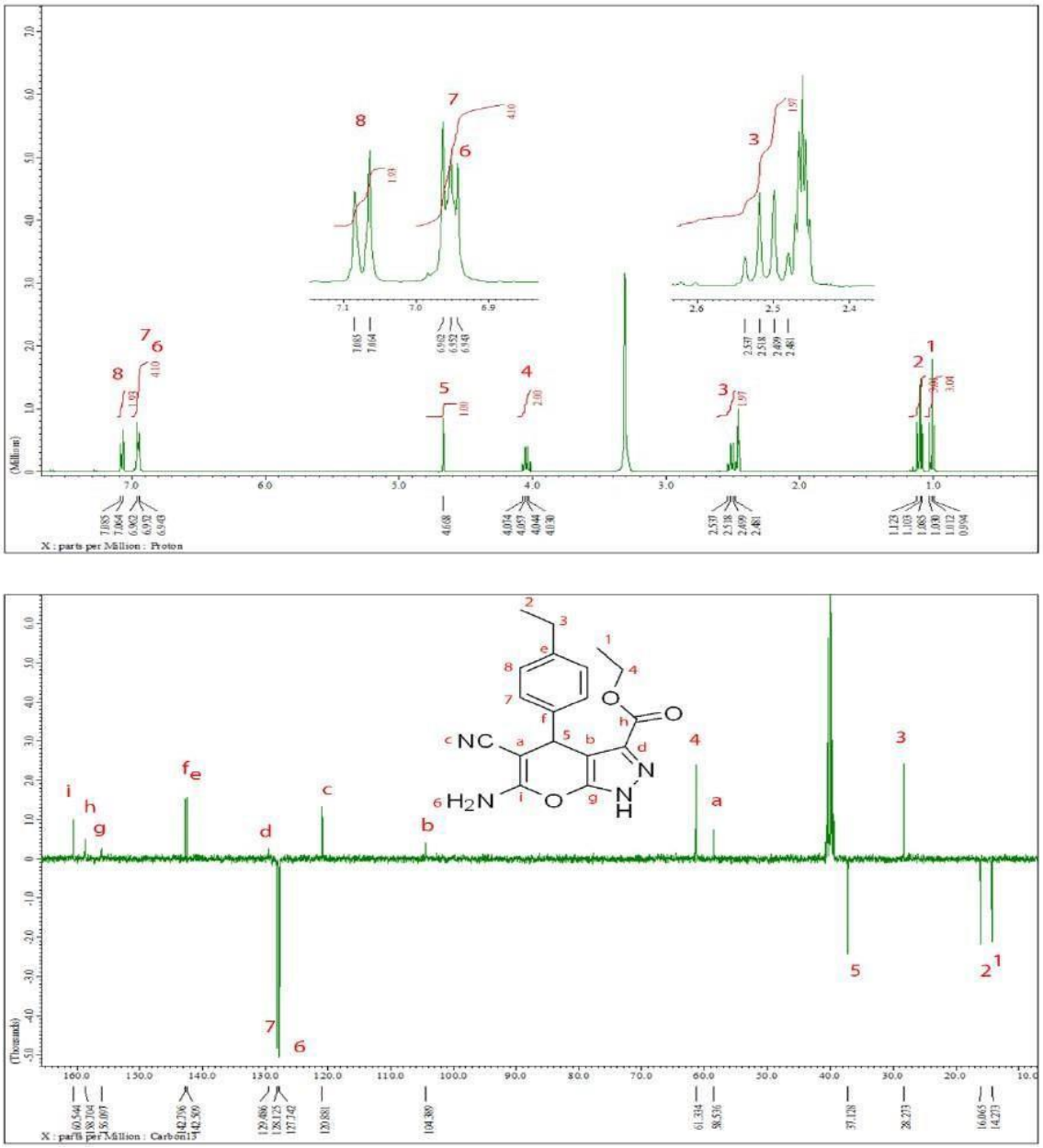

Figure 5. ^{1}H (400 MHz, DMSO-d_6) and ^{13}C-NMR (100 MHz, $CDCl_3$) spectra of compound **1b**

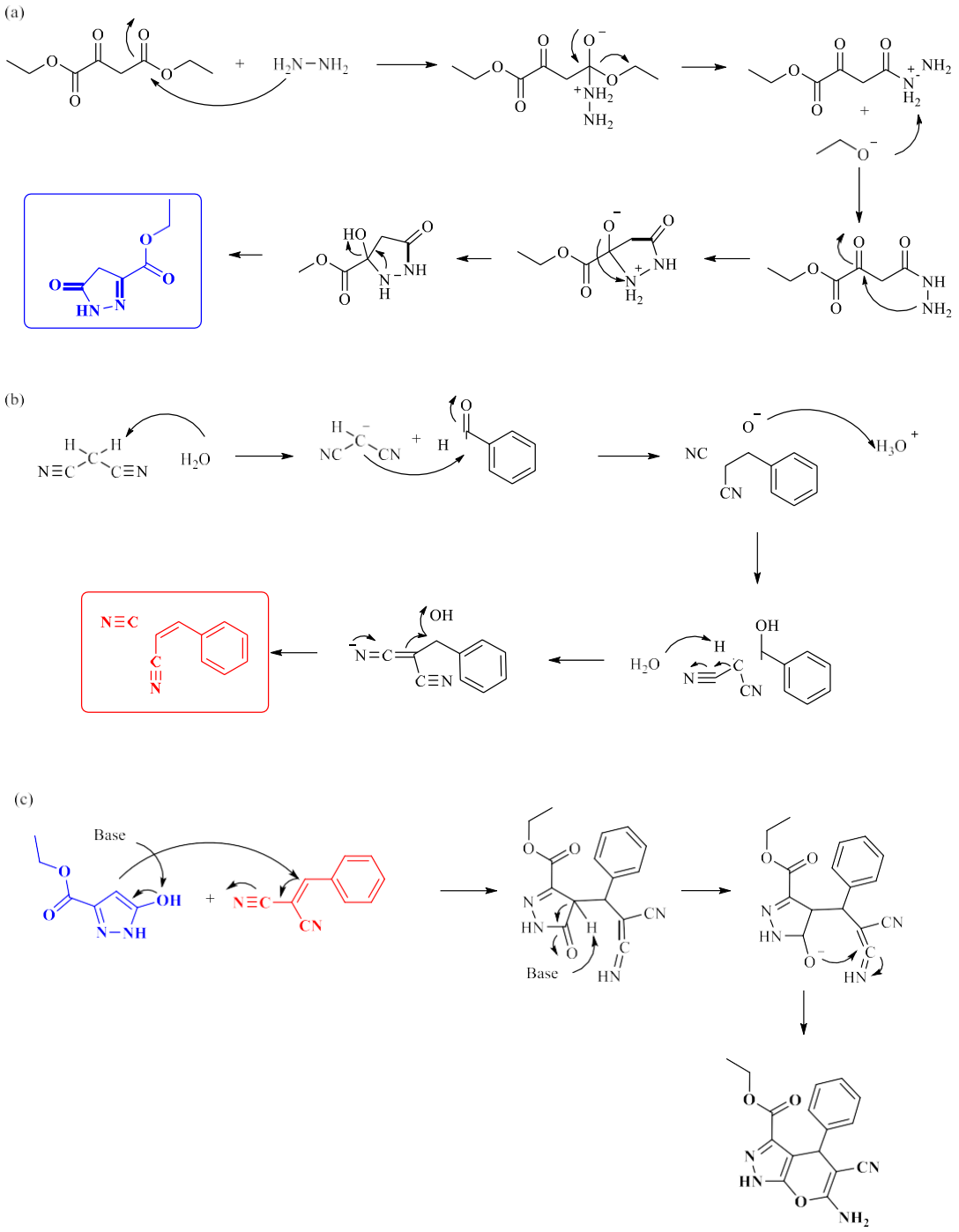

Figure 6. The reaction mechanism of compound **1a** comprising two parallel reactions leading to the formation of pyrazolone (blue box) and 2-benzylidenemalonodinitrile (red box) intermediates

Molecular docking studies are essential for discovering new antimalarial drugs that offer more practicality and less expensive. The enzyme of glycolytic pathways has been investigated as a promising molecular drug target due to its function in catalyzing pyruvate's interconversion to lactate for energy production in living cells [17]. Malarial parasites degrade hemoglobin to hematin, which then intoxicates the parasites by competing with NADH for the active site of *Pf*LDH. The inhibition of heme polymerization causes parasite death [18]. The analogs of pyrano[2,3-c]pyrazoles as potential inhibitors of *Pf*LDH were docked on the crystallized X-ray structure of *Pf*LDH to study the *in silico* interaction of the compounds with the enzyme. The docking results were expressed in terms of binding affinity in kcal/mol. Potentials binding sites for the compounds and cofactor binding sites could be identified in the molecular docking of *Pf*LDH. The tested (**1a-e**) compounds showed less docking scores than the crystalized NADH cofactor when docked, as summarized in **Table 1**. The tested compounds were relatively weaker when compared with the activity of co-crystal ligands NADH (which has docking energy

of -101.708 kcal/mol), which could be ranked in order of compound **1b** (highest at -36.4735 kcal/mol**)** followed by compound **1a** (-34.5383 kcal/mol), **1d** (-34.4910 kcal/mol), **1c** (-34.2995 kcal/mol), and **1e** (lowest at -33.6390 kcal/mol). This observation shows that these compounds do not inhibit *Pf*LDH from producing energy. The hydrogen bonds between each compound and the *Pf*LDH active site are also shown in **Table 1**, five hydrogen bonds. A hydrogen bond interaction was observed between the amine group of **1b** and oxygen of the side chain of Asp53. **Figure 7** shows the 2D and 3D binding poses of compound **1b** in the active site pocket of *Pf*LDH.

The *in silico* evaluation of ADMET characteristics plays a significant role in the drug design process before pursuing potential drug candidates with relevant pharmacokinetic, metabolic, and toxicity properties. All the data for ADMET properties are tabulated in **Table 2**. High polarity drugs do not penetrate the blood-brain barrier (BBB). The central nervous system (CNS) is evaluated based on the value of predicted central nervous system (CNS) which is -2(inactive) to +2 (active). In the present study, the value for all compounds was -2 (inactive), in which all of the compounds have low or absent CNS side effects. Hence the compounds may not be able to cross the blood-brain barrier. The HERG K^+ channel is a group of the Ether-a-go-go family encoded by the $KCHNH_2$ gene that contains four similar subunits [19]. This channel has been recognized to be a significant part of the heart's electrical activity that coordinates the heart's beating. This channel also appears to evaluate the cardiac toxicity of various therapeutic drugs [20]. Thus, a HERG K^+ channel blocker is possible to be toxic, and the IC_{50} value usually gives a reasonable estimation of cardiac toxicity [21]. In this study, the cardiac toxicity was determined by the estimated IC_{50} value for the blockage of this channel. The estimated log IC_{50} value for the blockage of HERG K^+ channels (log HERG) should be >-5. It was found that all the compounds were in the recommended range.

Table 1. Docking results for compounds **1a-e** inside *Pf*LDH

Compound	Binding affinity (kcal/mol)	Residues of the NADH binding site responsible for interaction with the compounds
1a	-34.5383	Thr97, Asp53, Ile31, Ser28, Gly27
1b	-36.4735	Thr97, Asp53, Ile31, Gly32, Thr101
1c	-34.2995	Thr97, Ile31, Ser28, Gly27
1d	-34.4910	Thr97, Gly99, Asn140, Ser245, Pro246
1e	-33.6390	Gly99, Phe100, Ser245, Gly32, Gly29
NADH	-101.708	Asn140, Phe100, Thr97, Val138, Leu163, Ile31 Gly99, Met30, Asp53, Thr139

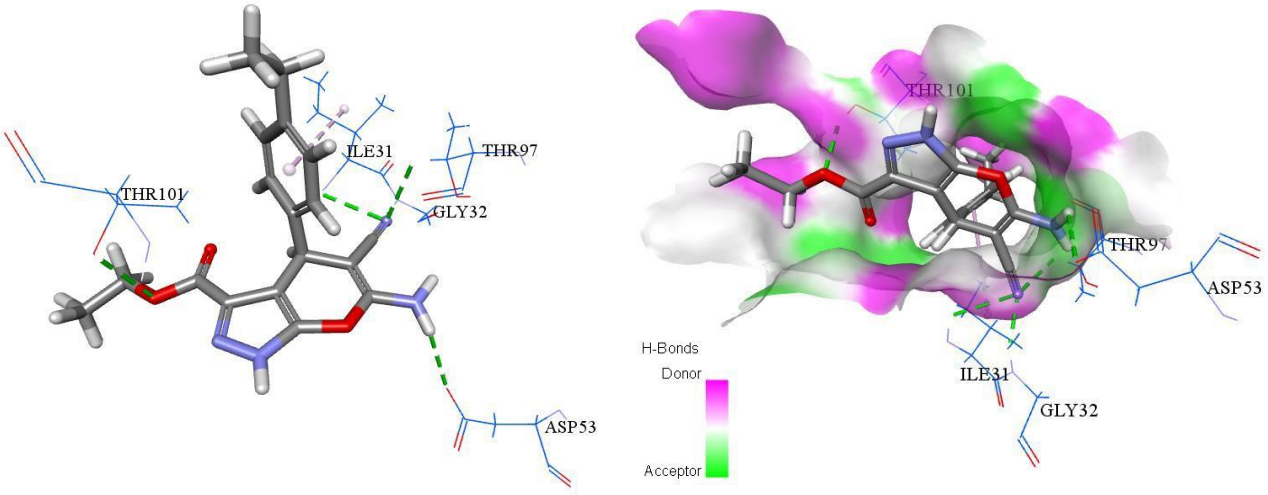

Figure 7. 2D and 3D binding modes of compound **1b** with an essential amino acid residue of *Pf*LDH. The atoms' coloring for the compound is in the following scheme: carbon in black, oxygen in red, and hydrogen in white. The green line indicates the hydrogen bonding interaction.

Table 2. Analysis of ADMET properties of dihydropyrano[2,3-c]pyrazole-3-carboxylate using GLIDE program

Compound	CNS	QP log HERG	Human oral absorption	Percentage of human oral absorption
1a	-2	-4.877	3	74.424%
1b	-2	-4.159	3	75.003%
1c	-2	-4.152	3	63.085%
1d	-2	-3.837	3	70.158%
1e	-2	-4.602	2	57.499%

CNS score – predicted central nervous system (-2 inactive; +2 active)
Percentage human absorption – predicted human oral absorption (>80% is high; <25% is low)
QP log HERQ – predicted IC_{50} value for the blockage of HERG K^+ channels (concern below -5)

Table 3. Evaluation of Lipinski's rule of five for compounds **1a-e**

Compound	Log p (lipophilicity)	Hydrogen bond donor <5	Hydrogen bond acceptor <10	Molecular weight < 500 g/mol
1a	2.22	3	5	294.0
1b	2.78	3	5	322.0
1c	1.81	3	6	284.0
1d	1.82	3	5	260.0
1e	1.92	4	6	310.0

Lipinski's rule of five is an empirical rule of thumb to evaluate physicochemical properties and refine small molecules' drug ability. This evaluation is beneficial to predict drug-likeliness characteristics of designed compounds. All test compounds appeared to adhere to all the rules, which could be preliminarily classified as drug-like [22, 23]. As shown in **Table 3**, the results revealed that compounds **1a-e are** composed of no more than five hydrogen bond donors and ten hydrogen bond acceptors. The increasing number of hydrogen bonds may reduce partitioning from the aqueous phase into the lipid bilayer membrane permeation by passive diffusion. Besides, the compounds' molecular mass also appeared to be less than 500 Daltons. An increase in molecular weight may reduce the compound concentration at the intestinal epithelium's surface, hence lessens the absorption. The lipophilicity of compounds **1a-e** was also less than five, thus could prevent low absorption or permeation [23]. From here, it can be suggested that compounds **1a-e** pose acceptable drug-likeliness behavior favorable for membrane permeability with desired drug-receptor interaction.

CONCLUSION

Five pyrano[2,3-c]pyrazole-3-carboxylates were successfully synthesized and characterized using spectral analyses. The molecular docking studies indicated that the compounds have lower binding affinity than NADH, thus are not capable of inhibiting *Pf*LDH for energy production. Nevertheless, the ADMET data suggested that the studied compounds have low or absent central nervous system side effects. Hence, the compounds may not be able to cross the blood-brain barrier. The cardiac toxicity determined by the estimated IC_{50} value for the HERG K+ channel blockage showed that these derivatives were within the recommended range. Moreover, the compounds successfully passed the rule of five, suggesting that the compounds hold the potential of becoming orally active drugs. The utilization of molecular hybridization with quinoline moiety is currently being investigated to improve the interaction in the active site of *Pf*LDH.

ACKNOWLEDGEMENT

The authors wish to thank the Ministry of Higher Education, Malaysia for providing funds for the research work (FRGS/1/2019/STG01/UKM/02/3) and Organic Synthesis Laboratory, Institute of Science, Puncak Alam Campus, Universiti Teknologi MARA for providing necessary laboratory facilities and technical assistance.

REFERENCES

1. Manohar, S., Khan, S. I. and Rawat, D. S. (2010) Synthesis, antimalarial activity, and cytotoxicity of 4-aminoquinoline-triazine conjugates. *Bioorganic and Medicinal Chemistry Letters*, **20(1)**, 322–325.

2. Hasan, A., Mazumder, H. H., Chowdhury, A. S., Datta, A. and Khan, A. (2015) Molecular-docking study of malaria drug target enzyme transketolase in *Plasmodium falciparum* 3D7 portends the novel approach to its treatment. *Source Code for Biology and Medicine*, **10(7)**, 1–14.

3. Sandeep, S. and Shailja, S. (2014) A brief history of quinoline as antimalarial agents. *International Journal of Pharmaceutical Sciences Review and Research*, **25(1)**, 295–302.

4. Preuss, J., Jortzik, E. and Becker, K. (2012) Glucose-6-phosphate metabolism in *Plasmodium falciparum*. *IUBMB Life*, **64(7)**, 603–611.

5. Shadrack, D. M., Nyandoro, S. S., Munissi, J. J. E. and Mubofu, E. B. (2016) In silico evaluation of antimalarial agents from hoslundia opposite as inhibitors of *Plasmodium falciparum* lactate dehydrogenase (*Pf* LDH) enzyme. *Computational Molecular Bioscience*, **06(02)**, 23–32.

6. Waingeh, V. F., Groves, A. T. and Eberle, J. A. (2013) Binding of quinoline-based inhibitors to *Plasmodium falciparum* lactate dehydrogenase: a molecular docking study. *Open Journal of Biophysics*, **3(4)**, *285–290.*

7. Read, J. A., Wilkinson, K. W., Tranter, R., Sessions, R. B. and Brady, R. L. (1999) Chloroquine binds in the cofactor binding site of *Plasmodium falciparum* lactate dehydrogenase. *The Journal of Biological Chemistry*, **274(15)**, 10213–10218.

8. Al-bayati, R. I. H., Saed, F. M., and Ali, W. B. (2011) Synthesis of new pyranopyrazole derivatives. *Al-Mustansiriyah Journal of Science*, **22(4)**, 166–174.

9. Al-amiery, A. A., Al-bayati, R. I., Saed, F. M., Ali, W. B., Kadhum, A. A. H. and Mohamad, A. B. (2012) Novel pyranopyrazoles: synthesis and theoretical studies. *Molecules*. **17(9)**, 10377–10389.

10. Kiyani, H., Samimi, H. A., Ghorbani, F. and Esmaieli, S. (2013) One-pot, four-component synthesis of pyrano[2,3-c]pyrazoles catalyzed by sodium benzoate in aqueous medium. *Current Chemistry Letters*, **2**, 197–206.

11. Sonar, J. P., Pardeshi, S. D., Dokhe, S. A., Zine, A. M., Pawar, R. P. and Thore, S. N. (2018) An efficient protocol for the one-pot synthesis of pyranopyrazoles in aqueous medium using triethanolamine as a catalyst. *Archives of Organic and Inorganic Chemical Sciences*, **3(1)**, 3–6.

12. Mohammat, M. F., Maarop, M. S., Shaameri, Z., Wibowo, A. Johari, S. A. and Hamzah, A. S. (2018) Practical synthesis and electronic study of non-piro and spiropyrano[2,3-c]pyrazole-3-carboxylate derivatives via uncatalyzed domino one-pot, four-component reaction, *Organic Communications*, **11(3)**, 149–162.

13. Shrivastava, A., Kumar, J., and Alam, M. M. (2016) In-silico assessment of various PDB entries of *Pf*LDH enzyme for their use in SBDD. *Chemical Informatics*, **2(12)**, 1–9.

14. Syahri, J.; Nurohmah, B. A.; Yuanita, E.; Armunanto, R.; Purwono, B. (2017) Chalcone analogue as potent antimalarial compounds against *Plasmodium falciparum*: synthesis, biological evaluation, and docking simulation study. *Asian Pacific Journal of Tropical Biomedicine*, **7(7)**, 1–5.

15. Jayaram, B., Tanya, S., Goutam, M., Abhinav, M., Shashank, S. and Vandana, S. (2012) Sanjeevini: a freely accessible web-server for target-directed lead molecule discovery. *BMC Bioinformatics*, **13(17)S7**, 1-13.

16. Gein, V. L., Zamareva, T. M. and Kozuline, I. V. (2014) New synthesis of ethyl 6-amino-4-aryl-5-cyano-1,4-dihydropyrano[2,3-c]pyrazole-3-carboxylates. *Russian Journal of Organic Chemistry*, **50**, 691–693.

17. Penna-Coutinho, J., Cortopassi, W. A., Oliveira, A. A. França, T. C. and Krettli, A. U. (2011) Antimalarial activity of potential inhibitors of *Plasmodium falciparum* lactate dehydrogenase enzyme selected by docking studies. *Plos One*, **6(7)**, 21237.

18. Egan, T. and Ncokazi, K. (2005) Quinoline antimalarials decrease the rate of beta-hematin formation. *Journal of Inorganic Biochemistry*, **99(7)**, 1532–1539.

19. Chemi, G., Gemma, S., Campiani, G., Brogi, S., Butini, S. and Brindisi, M. (2017) Computational tool for fast in silico evaluation of hERG K^+ channel affinity. *Frontiers in Chemistry*, **5(2)**, 1–9.

20. Kratz, J. M., Schuster, D., Edtbauer, M., Saxena, P., Mair, C. E., Kirchebner, J., Matuszczak, B., Baburin, I., Hering, S. and Rollinger, J. M. (2014) Experimentally validated hERG pharmacophore models as cardiotoxicity prediction tools. *Journal of Chemical Information and Modeling*, **54(10)**, 2887–2901.

21. Ntie-Kang, F. (2013) An in silico evaluation of the ADMET profile of the StreptoemDB database. *Springer Plus*, **2(353)**, 1–11.

22. Lipinski, C. A., Lombardo, F., Dominy, B. W. and Feeney, P. J. (2001) Experimental and computational approaches to estimate solubility and permeability in drug discovery and development settings. *Advanced Drug Delivery Reviews*, **46(1-3)**, 3–26.

23. Kalita, J., Chetia, D. and Rudrapal, M. (2019) Molecular docking, drug-likeliness studies, and ADMET prediction of quinoline imines for antimalarial activity. *Journal of Medicinal Chemistry and Drug Design*, **2(1)**, 1–7.